

## Full Length Article

# Advanced exergy analysis and optimization of a CO<sub>2</sub> to methanol process based on rigorous modeling and simulation

Qingchun Yang<sup>a,b,\*</sup>, Zhi Zhang<sup>a</sup>, Yingjie Fan<sup>a</sup>, Genyun Chu<sup>a</sup>, Dawei Zhang<sup>a,\*</sup>, Jianhua Yu<sup>c</sup>

<sup>a</sup> School of Chemistry and Chemical Engineering, Hefei University of Technology, Hefei 230009, PR China

<sup>b</sup> Anhui HaoYuan Chemical Group Co., Ltd., Fuyang 236023, PR China

<sup>c</sup> State Grid Anhui Electric Power Co., Ltd., Guangde Power Supply Company, Guangde 242200, PR China

## ARTICLE INFO

## Keywords:

CO<sub>2</sub> to methanol  
Advanced exergy analysis  
Improvement potential  
Avoidable exergy destruction  
Simulation

## ABSTRACT

The efficient conversion and utilization of CO<sub>2</sub> is of great strategic significance to achieve the goal of “carbon neutrality”. The production of green methanol from the captured CO<sub>2</sub> of industrial tail gas and green hydrogen of renewable energy can not only effectively reduce carbon emissions, but also solve the problem of green hydrogen storage and transportation. Facing with the unsatisfactory thermodynamic performance of CO<sub>2</sub> to methanol (CTM) process, however, little literature has been reported on the systematic investigation of its thermodynamic performance to reduce its avoidable exergy destruction instead of spending wasted effort to reduce unavoidable one. This study conducted an advanced exergy analysis of the CTM process to ascertain its real improvement potential and interactions among the components. Results show that the real improvement potential of the CTM process is 46.55%. Most of the exergy destruction of the CTM process is endogenous, which accounts for 94.47% of the total exergy destruction. After combination of splitting the exergy destruction, it finds that the unavoidable endogenous exergy destruction of the CTM process has the largest proportion, 50.93%, followed by avoidable endogenous exergy destruction, 43.55%. Besides, several improvement strategies are proposed to reduce the avoidable exergy destruction, which indicate that the total exergy destruction of the improved CTM process is reduced by 14.78% and exergy efficiency is increased by 4.91%.

## 1. Introduction

The control of the greenhouse gas emissions is a major challenge facing mankind in the 21st century. The concentration of CO<sub>2</sub> has increased by 30 % from pre-industrial levels due to the increase consumption of fossil fuels, and the CO<sub>2</sub> emissions are predicted to reach about 26 billion tons/year in 2100 [1]. The continued increase in carbon emissions will cause detrimentally global environmental impacts, such as global warming, melting glaciers, abnormal climate, rising sea levels and submerging continents [2]. Therefore, carbon reduction is imperative and has become the common action of the whole world.

The Carbon Capture and Storage (CCS) is commonly suggested for large-scale reduction of greenhouse gas emissions, however, most of CCS projects is still in the research and development (R&D) or demonstration stage, and there are still prominent obstacles such as high energy consumption, high investment cost, and high risk of CO<sub>2</sub> leakage [3]. If the captured CO<sub>2</sub> was employed to produce high economic value-added chemicals, this technology would be economical or even greatly

profitable [4]. In this regard, catalytic hydrogenation of CO<sub>2</sub> is a more feasible approach with the most promising development perspective and a relatively high probability of being applied as a large-scale commercial technology in the near future [5].

Methanol is widely applied in the chemical industry as a crucial platform chemical to produce olefins, formaldehyde, acetic acid, dimethyl ether, methylamine, etc. [6] In addition, due to methanol has good combustion properties, it can be used as a fuel in vehicles, which make methanol considered as a viable alternative energy source [7]. Hence, this study focuses on the catalytic hydrogenation of CO<sub>2</sub> to methanol process. Due to the water electrolysis hydrogen production technology derived from renewable energy sources does not rely on carbon-containing resources such as fossil fuels, and the technology is employed to supplement the hydrogen required for the CO<sub>2</sub>-to-methanol (CTM) process.

However, most of the reported literature is conducted by the chemistry and catalysis researchers and focuses on the development of catalysts for CO<sub>2</sub> to methanol [8–11], the exploration of the reaction mechanism [12–14] and kinetic [15–16] of CTM reaction. Several

\* Corresponding authors at: School of Chemistry and Chemical Engineering, Hefei University of Technology, Hefei 230009, PR China.

E-mail addresses: [ceqcyang@hfut.edu.cn](mailto:ceqcyang@hfut.edu.cn) (Q. Yang), [zhangdw@ustc.edu.cn](mailto:zhangdw@ustc.edu.cn) (D. Zhang).

<https://doi.org/10.1016/j.fuel.2022.124944>

Received 13 April 2022; Received in revised form 2 June 2022; Accepted 16 June 2022

Available online 23 June 2022

0016-2361/© 2022 Elsevier Ltd. All rights reserved.

Nomenclature			
$K$	pre-exponent factor	$E_{F,i}$	exergy of fuel of $i^{\text{th}}$ component
$T$	temperature	$E_{P,i}$	exergy of product of $i^{\text{th}}$ component
$n$	temperature exponent	$E_{D,i}$	exergy destruction of $i^{\text{th}}$ component
$E_a$	activation energy	$\varepsilon_i$	exergy destruction of $i^{\text{th}}$ component
$R$	universal gas law constant	$y_i$	exergy destruction ratio of $i^{\text{th}}$ component
$C$	concentration	<b>Abbreviations</b>	
$\nu$	concentration exponent	CTM	CO <sub>2</sub> to methanol
$K_i^{\text{eq}}$	equilibrium constant of reactions	CCS	Carbon Capture and Storage
$F$	fugacity	EN	endogenous
$E_{ph}$	physical exergy	EX	exogenous
$E_{ch}$	chemical exergy	UN	unavoidable
		AV	avoidable

reported works [17–19] have investigated the technical and economic performance of the CTM process. These works can advance the understanding of the CTM process; however, few published works have investigated the thermodynamic performance of the CTM process to further reduce system energy consumption and indirect carbon emissions.

Exergy-based analysis is an effective method and tool to address the above issues by determining the source, magnitude, and location of the exergy inefficiency of a system based on the exergy balance model of the system [20]. Wiesberg et al. [21] conducted a conventional exergy analysis of CTM process, and found that its exergy efficiency about 66.3 %. It indicates that CTM process has a relatively high improvement potential due to its large exergy destruction ratio. However, adopting the conventional exergy analysis method cannot determine the proportion of inefficiencies that can be avoided. Hence, it cannot identify the real improvement potential of a process [22]. Besides, conventional exergy analysis does not investigate the interactions between the components of a system. Thus, it cannot assess the effect of the ineffectiveness in one process on another [23]. Therefore, faced with the high exergy destruction ratio of the CTM process, how and where the energy/exergy is degraded? What are the effective measures to reduce avoidable exergy losses instead of spending wasted effort to reduce unavoidable exergy losses?

The advanced exergy analysis method is such a reliable and effective approach, which is superior to conventional exergy analysis by splitting exergy destruction into endogenous, exogenous, unavoidable and avoidable parts. In this regard, it can provide more detailed exergy destruction information for improving energy conversion system, and identify the possible misleading results obtained from the conventional method [24]. For example, Yuan et al. [25] applied advanced exergy analysis to determine the energy saving potential of an industrial ethylene cracking furnace. The results show that the combustion and reaction processes have the highest unavoidable and avoidable exergy destruction. Wu and Wang [26] found that 57.99 % and 86.07 % of total exergy destruction of the coal-to-SNG process is avoidable and endogenous based on advanced exergy analysis. Song et al. [24] quantified the real improvement potential of the proposed solid oxide fuel cell system by adopting the advanced exergy analysis method. They found that only 48.39 % of the total exergy destruction of the proposed system can be avoidable, and 87.50 % of the total exergy destruction is mainly related to the component itself. The results of advanced exergy analysis indicate, in the SOFC system, the Stack should be given the priority for optimization because it has the highest avoidable exergy destruction. However, to the best of our knowledge, few literatures have reported on the advanced exergy analysis of the CO<sub>2</sub> to methanol process to identify its real improvement potential and determine the interdependencies between the components, which are important to seek for the effective improvement measures.

Therefore, the main contributions of this work are: (a) to ascertain

the material flow and energy flow of the CTM process through the rigorous modeling and simulation of the entire process; (b) to determine the exergy destruction of each components of the CTM process by performing a conventional exergy analysis; (c) to further identify the endogenous, exogenous, avoidable, and unavoidable exergy destructions of the CTM process through advanced exergy analysis; (d) to find the most effective measures in terms of the endogenous and exogenous avoidable exergy destructions through parametric optimization; and (e) to compare the thermodynamic performance of the improved and referenced CTM process based on the results of the key parameters optimization.

## 2. Process description

The CTM process is a typical reaction-separation-recycle process as shown in Fig. 1. The carbon dioxide captured from industrial flue gas and the hydrogen generated by electrolysis of water from renewable energy sources are selected as the raw material for methanol production. The mixture of CO<sub>2</sub> and H<sub>2</sub> gases is then pressured and heated to 5–10 MPa and 200–300 °C before entering the methanol synthesis reactor. In the reactor, CO<sub>2</sub> is reacted with H<sub>2</sub> to produce methanol as shown in Eq. (1). Besides, there are also two parallel reactions in the methanol synthesis reactor as shown in Eqs. (2) and (3). Since the reaction is an exothermic reaction, this process adopts 0.41 MPa saturated deoxygenated water to remove the heat of the reactor in time. The output of the reactor contains products (CH<sub>3</sub>OH and H<sub>2</sub>O) and unreacted raw gases (H<sub>2</sub>, CO<sub>2</sub> and CO) because of the chemical equilibrium limitations. Therefore, a gas–liquid flash is employed to separate unreacted gas from methanol. Most of the output gas of the flash is recycled to the methanol synthesis reactor to increase the conversion of reactants; and the rest is as the tail gas to avoid high content of inert gases. The liquid stream out from the flash is sent to a separation column and a distillation column. The former is used to remove the light gas from the methanol stream; and the latter is typically a distillation column to obtain high-purity methanol product.



## 3. Methodology

To quantify the real improvement potential and interdependencies among the components and the whole CTM process, the workflow for the advance exergy analysis of the CTM process is shown in Fig. 2.

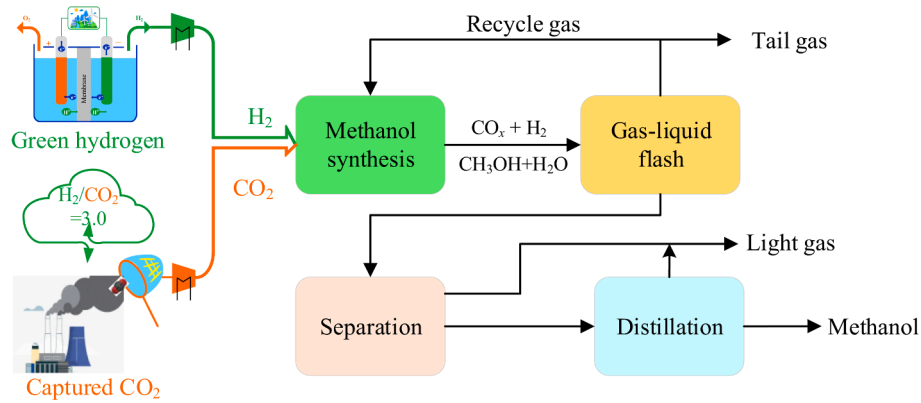


Fig. 1. Block diagram of CO<sub>2</sub> hydrogenation to methanol process.

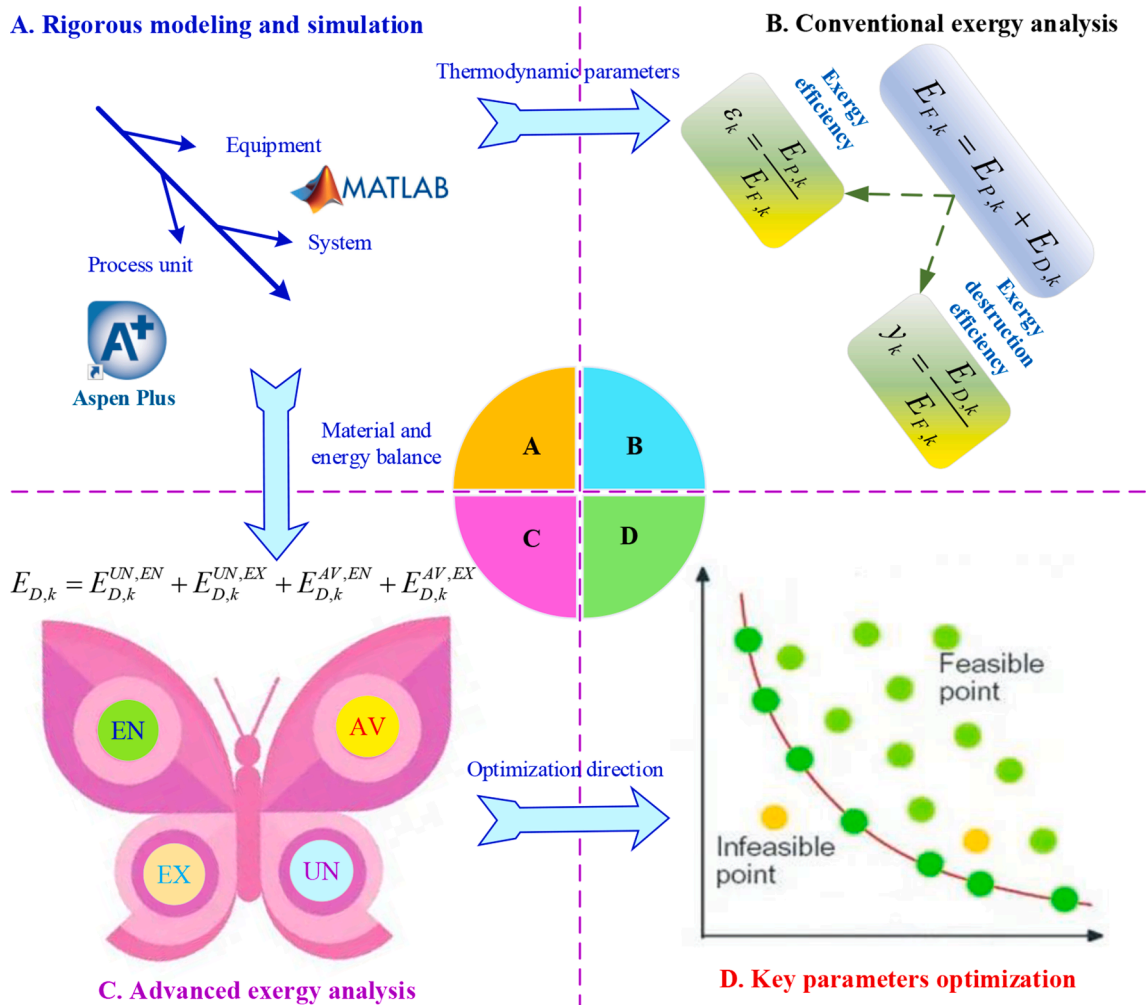


Fig. 2. Overview of the research method of this study.

- A. Rigorous modeling and simulation:** It is to build the equipment, process unit and system models of the CTM for calculating the material and energy balance.
- B. Conventional exergy analysis:** It is to establish the exergy balance of the components and whole system for determine the exergy efficiency and exergy destruction of the CTM process.
- C. Advanced exergy analysis:** It is to further identify the essential causes and real improvement potential of exergy destruction by

splitting into endogenous (EN), exogenous (EX), unavoidable (UN), and avoidable (AV) parts.

- D. Key parameters optimization:** It is to investigate the effect of the key parameters on the avoidable exergy destruction from the endogenous and exogenous perspectives to provide theoretical basis and technical support for subsequent system improvement.
- E. Development of improvement strategies:** It is to make effectively measures to reduce endogenous and exogenous avoidable exergy destruction in term of the results of the above steps.

### 3.1. Rigorous modeling and simulation of the CTM process

The model of the CTM process is established using the simulator, Aspen Plus software, which is regarded as one of the most common used process modeling and simulation software for plant design, steady-state simulation and optimization [27]. The Redlich-Kwong-Soave (RK-SOAVE) property method is selected as the global property method for most of the components are non-polar or less polar substances, and the non-random two-liquid (NRTL) method is applied as the complementary property method of the crude methanol distillation process because of liquid methanol and water. The main assumptions for the modeling and simulation of the CTM process are indicated as follows:

- (1) The CTM system is operated in a steady-state, and all parameters do not change with time;
- (2) The pressure drop is mainly set in the equipment, and there is no pressure drop in the mixer model and piping;
- (3) The material in the methanol reactor moves forward in parallel along the movement direction, and the flow velocity is equal everywhere along the radial direction;
- (4) The components of the CTM system are mainly composed of  $H_2$ ,  $CO_2$ ,  $CO$ ,  $H_2O$  and  $CH_3OH$  due to the amount of other substances is negligible.

The whole simulation flowsheet of the CTM process is indicated in Fig. 3. More detailed parameters for the modeling and simulation are shown in Table 1. The captured CO<sub>2</sub> is firstly mixed with the recycle gas and then preheated in a HeatX model, which is defined as 8 MPa and vapor fraction equalled to one. The mixture stream (M2) is heated to 250 °C in a Heater model. The outlet of the heater is sent to the methanol synthesis reactor, which is modeled by a kinetic based reactor model, RPlug model. The commercial Cu/ZnO/Al<sub>2</sub>O<sub>3</sub> catalyst is employed in this work because of relatively high performance [28]. Due to the kinetic rate expressions developed by Graaf cannot be directed used in the software, it is improved in the built-in form as follows [29]:

$$r = \frac{[\text{Kinetic factor}][\text{Driving force}]}{[\text{Adsorption term}]} \quad (4)$$

An Arrhenius term and a pre-exponent factor are used to specify the kinetic factor as follows:

$$\text{Kinetic factor} = kT^n e^{(-\frac{E_g}{KT})} \quad (5)$$

where  $k$ ,  $T$ ,  $n$  denote pre-exponent factor, temperature, and temperature

Table 1

Detailed parameters for the modeling and simulation of the CTM process.

	Full name	Aspen model	Key input parameters
HX	Heat exchanger	HeatX	$T_{\text{hot, out}} = 120^{\circ}\text{C}$
EX6	Heater	Heater	$T = 200^{\circ}\text{C}$ ; $P = 8 \text{ MPa}$
R	Methanol synthesis reactor	RPlug	$T = 200^{\circ}\text{C}$ ; $P = 8 \text{ MPa}$ ; catalyst loading = 865 kg; bed porosity = 0.3; Pipe diameter = 0.06 m
EX5	Heater	Heater	$T = 31^{\circ}\text{C}$ ; $P = 5 \text{ MPa}$
F1	Gas-liquid flash	Flash	$T = 30^{\circ}\text{C}$ ; $P = 5 \text{ MPa}$
FS	Splitter	FSplit	Fraction of TG1 stream = 0.02
CP5	Recycle compressor	Compr	$P = 8 \text{ MPa}$ ; isentropic efficiency = 0.72
STR	Stripper	RadFrac	Stage = 4; No reboiler or condenser
F2	Condenser	Flash	$T = 30^{\circ}\text{C}$ ; $\Delta P = 0$
F3	Low pressure flash	Flash	$Q = 0$ ; $P = 2 \text{ MPa}$
RAD	Methanol distillation	RAD	Stage = 30; $R = 0.73$ ; reboil ratio = 1.60
MC	Multistage compressor	MCompr	Number = 4; pressure = 0.3/0.9/2.77.6 MPa
EX4	Heater	Heater	$T = 170^{\circ}\text{C}$ ; $P = 7.5 \text{ MPa}$
MX	Mixer	Mixer	Default

exponent, respectively;  $E_a$  and  $R$  are activation energy and universal gas law constant. The temperature exponent is set to be zero in term of the work of Kiss et al. [7], and the rest parameters of the kinetic factor are indicated in Table 2.

The generalized form of driving force in the Aspen Plus is shown in Eq. (6). Due to the reactive phase is set as the vapor-only phase, the partial pressure of each component of the reactions are used to substitute concentration if the difference between fugacity and partial pressure is neglected. In this regard, the Aspen Plus built-in driving force expressions of reactions (1)-(3) are written as in Eqs. (7)-(9) [7]. The parameters of the driving force expressions are listed in Table 3, and changed into a logarithmic form by Eq. (10) for direct use in Aspen Plus.

Table 2

Input parameters of the kinetic factor of reactions (1)-(3) [7].

Reaction No.	k	E <sub>a</sub> (J/mol K)
1	$9.0421 \times 10^8 (\text{kmol/kg}_{\text{cat}} \text{ s Pa}^{1/2})$	112,860
2	$4.0638 \times 10^{-6} (\text{kmol/kg}_{\text{cat}} \text{ s Pa})$	11,695
3	$1.5188 \times 10^{-33} (\text{kmol/kg}_{\text{cat}} \text{ s Pa})$	266,010

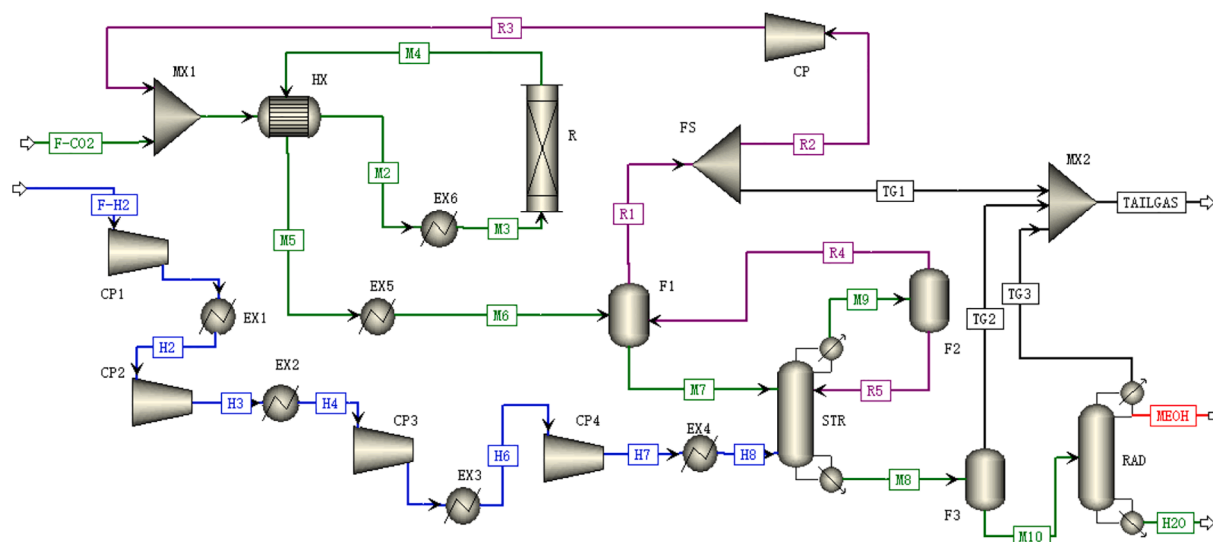


**Fig. 3.** Simulation flowsheet of the CTM process.

**Table 3**

Driving force constants of reactions (1)–(3).

Reaction	Expression $K_1$	$K_1$	$A^a$	$B^a$
1	$K_{CO_2} [\text{Pa}^{-1}]$	$1.7214 \times 10^{-10} \exp(81287/RT)$	−22.48	9777
2	$K_{CO} [\text{Pa}^{-1}]$	$8.3965 \times 10^{-11} \exp(118270/RT)$	−23.20	14,225
3	$K_{CO_2} [\text{Pa}^{-1}]$	$1.7214 \times 10^{-10} \exp(81287/RT)$	−22.48	9777
Reaction	Expression $K_2$	$K_2$	$A^a$	$B^a$
1	$K_{CO_2}/K_1^{eq} [\text{Pa}]$	$2.5813 \times 10^{10} \exp(26788/RT)$	23.974	3222
2	$K_{CO_2}/K_2^{eq} [\text{Pa}^{-1}]$	$6.1221 \times 10^{-13} \exp(125226/RT)$	−28.12	15,062
3	$K_{CO}/K_3^{eq} [\text{Pa}]$	$3.5408 \times 10^{12} \exp(19832/RT)$	28.895	2385

a: Logarithm of the driving force constant for Aspen Plus:  $A = \ln k$  and  $B = \ln E_a$ .

$$\text{Driving force} : K_1 \left( \prod C_i^{\nu_i} \right) - K_2 \left( \prod C_j^{\nu_j} \right) \quad (6)$$

$$\text{For reaction 1} : K_{CO_2} f_{CO_2} f_{H_2}^{1.5} - \frac{K_{CO_2}}{K_1^{eq}} f_{H_2O} f_{MeOH} f_{H_2}^{-1.5} \quad (7)$$

$$\text{For reaction 2} : K_{CO_2} f_{CO_2} f_{H_2} - \frac{K_{CO_2}}{K_2^{eq}} f_{H_2O} f_{CO} \quad (8)$$

$$\text{For reaction 3} : K_{CO} f_{CO} f_{H_2}^{1.5} - \frac{K_{CO}}{K_3^{eq}} f_{MeOH} f_{H_2}^{-0.5} \quad (9)$$

$$\text{Logarithm of the driving force constant} : \ln(K) = A + \frac{B}{T} \quad (10)$$

where  $C$  denotes the concentration;  $\nu$  means the concentration exponent;  $K_1^{eq}$ ,  $K_2^{eq}$  and  $K_3^{eq}$  represent the equilibrium constant of reactions (1)–(3), respectively; and  $f$  is the fugacity.

The adsorption term is expressed in a generalized form for all chemical reactions in Aspen Plus as shown in Eq. (11). According to the previous work of Kiss et al. [7], the adsorption term of the reactions (1)–(3) are the same as shown in Eq. (12). The input parameters of these adsorption expressions are summarized in Table 4.

$$\text{Adsorption term} : \left[ \sum K_i \left( \prod C_j^{\nu_j} \right) \right]^m \\ = [\text{Term 1} + \text{Term 2} + \dots + \text{Term } n]^m \quad (11)$$

$$K_1 f_{H_2}^{0.5} + K_2 f_{H_2O} + K_3 f_{CO} f_{H_2}^{0.5} + K_4 f_{CO} f_{H_2O} + K_5 f_{CO_2} f_{H_2}^{0.5} + K_6 f_{CO_2} f_{H_2O} \quad (12)$$

$$\text{where } K_1 = 1; K_2 = \frac{K_{H_2O}}{K_{H_2}^{0.5}}; K_3 = K_{CO}; K_4 = \frac{K_{CO} K_{H_2O}}{K_{H_2}^{0.5}}; K_5 = K_{CO_2}; K_6 = \frac{K_{CO_2} K_{H_2O}}{K_{H_2}^{0.5}}.$$

The outlet of the methanol synthesis reactor is firstly sent for recovery of waste heat, and then fed into a flash (Flash2 Model) for separation of unreacted gas from methanol. The gaseous stream (R1) from the flash is recycled and mixed with fresh raw gas after the compression process. The liquid stream (M7) enters a stripping column where it is counter-current with the fresh hydrogen stream. The bottom of the stripping column enters a flash to remove light gas, and then fed into a distillation column to obtain high-purity methanol product. This column is modeled by a RadFrac model with a partial condenser.

**Table 4**

Resulting input parameters of the adsorption term of CTM reactions.

Term	$a_i$	$A_i = \ln(a_i)$	$b_i$	$B_i = b_i/R$	$\prod C_j^{\nu_j}$
1	$a_1 = 1$	0	$b_1 = 0$	0	$\sqrt{f_{H_2}}$
2	$a_2 = 4.3676 \times 10^{-12}$	−26.1568	$b_2 = 1.1508 \times 10^5$	13842&	$f_{H_2O}$
3	$a_3 = 8.3965 \times 10^{-11}$	−23.2006	$b_3 = 1.1827 \times 10^5$	14225	$f_{CO} \sqrt{f_{H_2}}$
4	$a_4 = 3.6673 \times 10^{-22}$	−49.3574	$b_4 = 2.3335 \times 10^5$	28067	$f_{CO} f_{H_2O}$
5	$a_5 = 1.7214 \times 10^{-10}$	−22.4827	$b_5 = 8.1287 \times 10^4$	9777	$f_{CO_2} \sqrt{f_{H_2}}$
6	$a_6 = 7.5184 \times 10^{-22}$	−48.6395	$b_6 = 1.9727 \times 10^5$	23619	$f_{CO} f_{H_2O}$

### 3.2. Conventional exergy analysis model

Exergy is the maximum useful work produced when the system reaches equilibrium with the environment. The exergy of a stream consists of physical and chemical exergy as follows:

$$E = E_{ph} + E_{ch} \quad (13)$$

where  $E_{ph}$  and  $E_{ch}$  are the physical and chemical exergy.

When the exergy of all streams of  $k^{\text{th}}$  component and the whole CTM system is determined, the exergy balance equations of the components and system are shown in Eqs. (14) and (15) in terms of the concepts of “Fuel -product” [30]:

$$E_{F,k} = E_{P,k} + E_{D,k} \quad (14)$$

$$E_{F,tot} = E_{P,tot} + E_{D,tot} + E_{L,tot} = E_{P,tot} + \sum E_{D,k} + E_{L,tot} \quad (15)$$

where  $E_{F,k}$ ,  $E_{P,k}$ ,  $E_{D,k}$ ,  $E_{F,tot}$ ,  $E_{P,tot}$ ,  $E_{D,tot}$ , and  $E_{L,tot}$  denote the exergy fuel, exergy product and exergy destruction of the  $k^{\text{th}}$  component and the whole system, respectively.

Exergy efficiency and exergy destruction ratio of the  $k^{\text{th}}$  component and the whole CTM process, which are the most important indicators to evaluate the thermodynamic performance of a system during convention exergy analysis, can be determined based on the above exergy balance equations as follows [31]:

$$\varepsilon_k = \frac{E_{P,k}}{E_{F,k}} \times 100\% = 1 - \frac{E_{D,k}}{E_{F,k}} \times 100\% \quad (16)$$

$$\varepsilon_{tot} = \frac{E_{P,tot}}{E_{F,tot}} \times 100\% = 1 - \frac{E_{D,tot}}{E_{F,tot}} \times 100\% \quad (17)$$

$$y_k = \frac{E_{D,k}}{E_{F,k}} \times 100\% \quad (18)$$

$$y_k^* = \frac{E_{D,k}}{E_{D,tot}} \times 100\% \quad (19)$$

$$y_{tot} = \frac{E_{D,tot}}{E_{F,tot}} \times 100\% \quad (20)$$

where  $\varepsilon_k$  and  $\varepsilon_{tot}$  stands for the exergy efficiency of the  $k^{\text{th}}$  component and the overall system;  $y_k$  and  $y_k^*$  and  $y_{tot}$  denote the ratio of the exergy



destruction within the  $k^{\text{th}}$  component to its total exergy of the fuel and to the total exergy destruction of the system; and  $y_{\text{tot}}$  means the ratio of the total exergy destruction to the total exergy of the fuel of the overall system [32].

### 3.3. Advanced exergy analysis model

Compared with conventional exergy analysis method, advanced exergy analysis method is a more powerful tool to further identify the sources of exergy destruction due to it can split exergy destruction into endogenous and exogenous as well as unavoidable and avoidable parts [33].

In the advanced exergy analysis, exergy destruction is divided into an endogenous and an exogenous part to investigate the interaction relationship among components as shown in Eqs. (21) and (22). The former part refers to the irreversibility occurring within the  $k^{\text{th}}$ -component itself, and latter part refers to the irreversibility causing by the interaction with the rest of the components [34].

$$E_{D,k} = E_{D,k}^{\text{EN}} + E_{D,k}^{\text{EX}} \quad (21)$$

$$E_{D,k}^{\text{EN}} = E_{P,\text{tot}}^{\text{real}} \left( \frac{E_{D,k}}{E_{P,\text{tot}}} \right)^{\text{EN}} \quad (22)$$

where  $E_{D,k}^{\text{EN}}$  and  $E_{D,k}^{\text{EX}}$  stand for the endogenous and exogenous exergy destruction.

Exergy destruction can be also divided into an unavoidable part and an avoidable part to demonstrate the real improvement potential of the component or the system as shown in Eqs. (23) and (24) [35]. The unavoidable exergy destruction cannot be further reduced because of the technical or economical limitations; and the avoidable exergy destruction can be reduced by improving the performance of the component.

$$E_{D,k} = E_{D,k}^{\text{AV}} + E_{D,k}^{\text{UN}} \quad (23)$$

$$E_{D,k}^{\text{UN}} = E_{P,k} \left( \frac{E_{D,k}}{E_{P,k}} \right)^{\text{UN}} \quad (24)$$

where  $E_{D,k}^{\text{UN}}$  and  $E_{D,k}^{\text{AV}}$  represent the unavoidable and avoidable exergy destruction.

According to the above concepts, the exergy destruction of  $k^{\text{th}}$  component can be split into four parts as written as follows [36]:

$$E_{D,k} = E_{D,k}^{\text{UN,EN}} + E_{D,k}^{\text{UN,EX}} + E_{D,k}^{\text{AV,EN}} + E_{D,k}^{\text{AV,EX}} \quad (25)$$

$$E_{D,k}^{\text{UN,EN}} = E_{P,k}^{\text{EN}} \times \left( \frac{E_D}{E_P} \right)_k^{\text{UN}} \quad (26)$$

$$E_{D,k}^{\text{UN,EX}} = E_{D,k}^{\text{UN}} - E_{D,k}^{\text{UN,EN}} \quad (27)$$

$$E_{D,k}^{\text{AV,EN}} = E_{D,k}^{\text{EN}} - E_{D,k}^{\text{UN,EN}} \quad (28)$$

$$E_{D,k}^{\text{AV,EX}} = E_{D,k}^{\text{EX}} - E_{D,k}^{\text{UN,EX}} \quad (29)$$

where  $E_{D,k}^{\text{UN,EN}}$ ,  $E_{D,k}^{\text{UN,EX}}$ ,  $E_{D,k}^{\text{AV,EN}}$  and  $E_{D,k}^{\text{AV,EX}}$  stand for the unavoidable endogenous, unavoidable exogenous, avoidable endogenous, and avoidable exogenous exergy destruction, respectively.

The  $E_{D,k}^{\text{UN,EN}}$  and  $E_{D,k}^{\text{UN,EX}}$  refer to the exergy destruction cannot be reduced because of technical or economical limitations of the  $k^{\text{th}}$  component and reduced by the other components of the overall system. The technical and economic limitations mainly include: (1) the exergy destruction that cannot be reduced because of the limitation of chemical equilibrium, the availability of materials or the manufacturing methods used; and (2) the exergy destruction that cannot be reduced because of the cost of equipment, materials or the manufacturing methods used. Hence, although the improvements are technically feasible, but they are

too costly to be economically viable. The  $E_{D,k}^{\text{AV,EN}}$  and  $E_{D,k}^{\text{AV,EX}}$  indicate the exergy destruction can be reduced by improving the efficiency of the  $k^{\text{th}}$  component and reduced by the rest components. The relationships of these different exergy destruction are indicated in Figure S1.

## 4. Results and discussion

### 4.1. Simulation results and validation

According to the rigorous models of the whole CTM process, the material and energy material balance results are obtained as shown in Tables S2 and S3 in the Supporting Information to shorten the length of the paper. It can be seen that 900 kmol/h  $\text{CO}_2$  and 2700 kmol/h  $\text{H}_2$  can finally produce methanol, 787.64 kmol/h with the molar fraction higher than 99.99 %. Due to the methanol synthesis reactor is the most important equipment, the simulation results of this reactor are compared with the experimental data as shown in Fig. 4. When most of the operational parameters of the methanol synthesis model are set as the same with those of the work by An et al. [37], the results show that the change trend of temperature on  $\text{CO}_2$  conversion and methanol yield is basically consistent with the experimental results. Thus, the established models and simulation results can be used for the following system analysis and optimization.

### 4.2. Implications of the conventional exergy analysis

According to the material and energy balance results, the exergy flow diagram of the CTM process is determined as shown in Fig. 5. The total input exergy of the CTM process is 235.2 MW, including raw material 183.9 MW, heat 25.7 MW, and electricity 25.6 MW, respectively. Because the unit chemical exergy of  $\text{CO}_2$  (20.075 kJ/mol) is much smaller than that of methanol (716.192 kJ/mol),  $\text{CO}$  (275.323 kJ/mol), and hydrogen (235.15 kJ/mol), the input exergy of  $\text{CO}_2$  stream is only 7.6 MW. Due to the low conversion ratio of  $\text{CO}_2$  hydrogenation reaction per pass, a large amount of unreacted gas needs to be recycled. Hence, 1405.6 MW unreacted gas are mixed with the fresh  $\text{CO}_2$  stream and then fed into the reactor. 164.2 MW crude methanol are separated from a flash tank and sent to a stripping tower to remove light gas. Finally, it can produce 156.7 MW high-purity methanol. Therefore, the total exergy efficiency of the CTM process is about 66.62 % as shown in Table 5.

As Table 5 shown, the exergy efficiency of all the components of the CTM process is higher than 90 % based on the concept of "Fuel-Product".

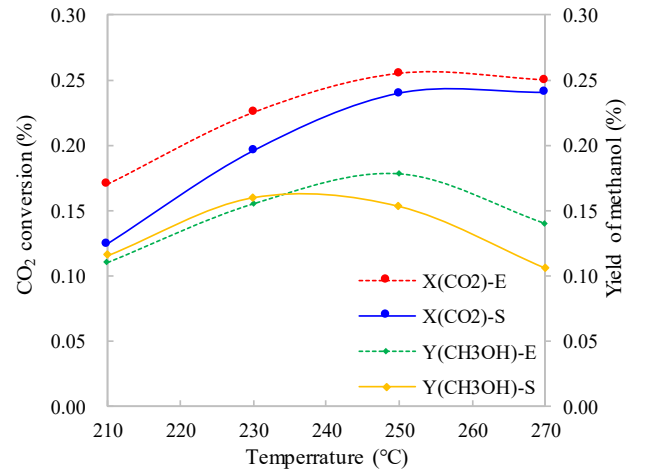


Fig. 4. Comparison of the simulation results (-S) and experiment data (-E) of reactor model.

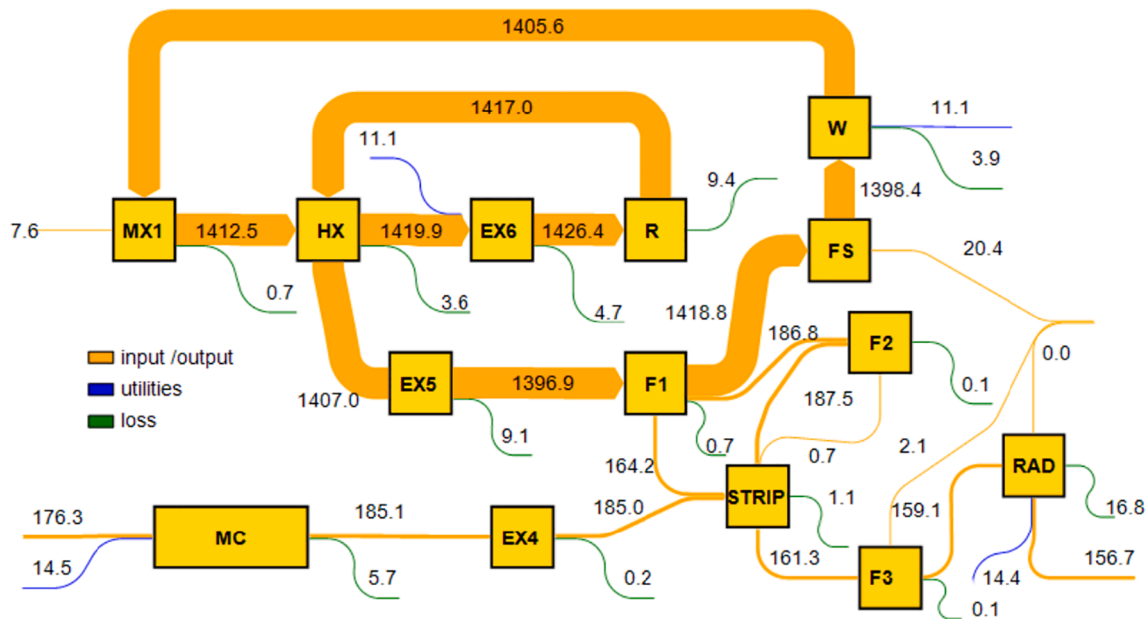


Fig. 5. Exergy flow of the CTM process (Unit of data: MW).

Table 5

Exergy efficiency and exergy destruction ratio of each component of the CTM process.

Component	$E_F$	$E_P$	$E_D$	$\varepsilon_k$	$\gamma_k$	$\gamma_k^*$
RAD	173.5	156.7	16.8	90.32	9.68	21.40
F3	161.3	159.1	2.2	98.64	1.36	2.80
STR	349.9	348.8	1.1	99.69	0.31	1.40
F1	1583.7	1583.0	0.7	99.96	0.04	0.89
F2	187.5	187.4	0.1	99.95	0.05	0.13
EX5	1406.0	1396.9	9.1	99.35	0.65	11.59
HX	2829.5	2825.9	3.6	99.87	0.13	4.59
R	1426.4	1417.0	9.4	99.34	0.66	11.97
EX6	1431.0	1426.4	4.6	99.68	0.32	5.86
FS	1418.8	1398.4	20.4	98.56	1.44	25.99
CP5	1409.5	1405.6	3.9	99.72	0.28	4.97
MX1	1413.2	1412.5	0.7	99.95	0.05	0.89
EX4	185.1	184.9	0.2	99.89	0.11	0.25
MC	190.8	185.1	5.7	97.01	2.99	7.26
Total	235.2	156.7	78.5	66.62	33.38	100

The distillation column, hydrogen multi-compressor, and splitter have the lowest exergy efficiency. It is mainly because that: (1) the distillation column consumes lots of additional utilities in the reboiler for maintaining the heating balance of the column; (2) the hydrogen multi-compressor contains a four-stage compressor resulting in a high irreversibility of the pressurization and cooling processes; (3) the splitter discharges a large amount of tail gas resulting in a low exergy efficiency if only considering the product exergy. As for the distributions of exergy destruction of the CTM process, it can be seen that the modified exergy destruction ratio ( $\gamma_k^*$ ) of the splitter is the largest, 25.99 %, followed by the distillation column, 21.40 %, and methanol synthesis reactor, 11.97 %. It means that these three components have the largest improvement potential. Three flash tanks and mixer of the CTM process, in comparison, have the lowest improvement potential.

Although the conventional exergy analysis method can determine the total exergy destruction of the component and the system, it cannot split them in depth. The exergy destruction ratio of the CTM process is high to 33.38 %, however, it is unclear how much is avoidable and how much is caused by interactions among the components of the CTM process.

#### 4.3. Implications of the advanced exergy analysis

The advanced exergy analysis method is applied to overcome the disadvantages of the conventional one. More detailed and useful information of the exergy destruction of the CTM process can be identified as follows.

##### 4.3.1. Endogenous and exogenous exergy destruction

Considering the interaction among the components of the CTM system, the exergy destruction of these components is divided into endogenous and exogenous parts as shown in Fig. 6. The results show that 94.47 % of the exergy destruction of the CTM process is endogenous exergy destruction. It means that most of exergy destruction are due to the irreversibility of the system's components themselves. The exergy destruction caused by the exogenous structure relationship among these components only accounts for 5.53 %. Thus, it should be paid more attention to improve the thermodynamic performance of the equipment of the CTM process. For example, the splitter, distillation column and methanol synthesis reactor have the largest proportion of the total endogenous exergy destruction, 26.88 %, 22.65 % and 12.02 %, respectively. These three components should be firstly optimized to reduce the exergy destruction of the CTM system.

##### 4.3.2. Unavoidable and avoidable exergy destruction

The avoidable exergy destruction of the CTM process is about 46.55 % as shown in Fig. 7. This means that the real improvement potential of the CTM process is 46.55 % for exergy destruction reduction. 53.45 % of the exergy destruction cannot be reduced for the currently technical or economic limitations. The splitter has the highest avoidable exergy destruction, 13.04 MW, followed by the distillation column, 6.80 MW, and the methanol synthesis reactor, 3.47 MW, respectively. Therefore, more efforts should be paid to reduce the avoidable exergy destruction of these three components.

##### 4.3.3. Combination of splitting the exergy destruction

The unavoidable endogenous exergy destruction of the CTM process has the largest proportion (50.93 %) of its total exergy destruction as indicated in Fig. 8(a). The  $E_{D,tot}^{UN,EN}$  of the CTM process is mainly caused by the distillation column (RAD), splitter (FS), and heat recovery cooler (EX5) as in Fig. 8(b). Hence, these components have the highest

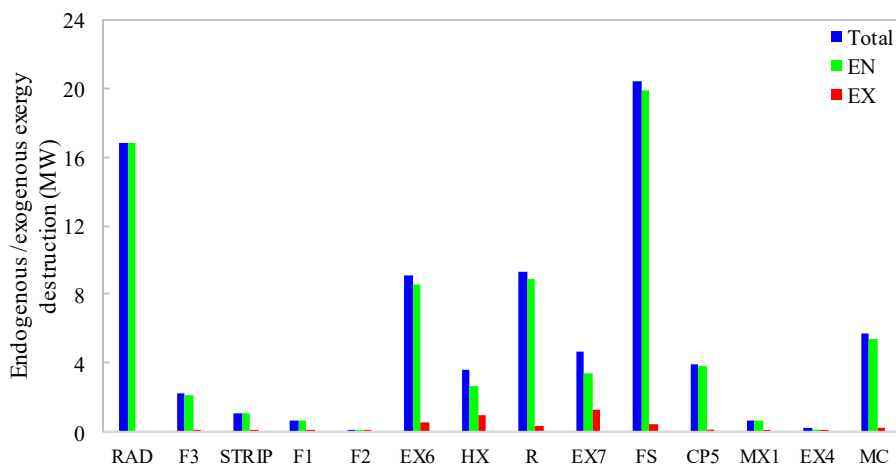


Fig. 6. Endogenous and exogenous exergy destruction of the CTM process.

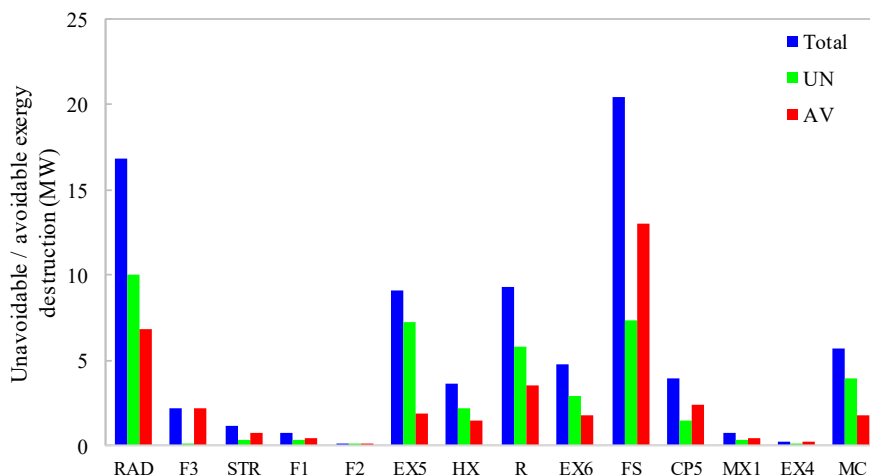


Fig. 7. Unavoidable and avoidable exergy destruction of the CTM process.

unavoidable endogenous exergy destruction which are limited to the irreversibility of the driving force of chemical reactions or the requirement of heat exchange temperature difference. They are not recommended to be reduced from the current state of the art or economic feasibility. The  $E_{D,tot}^{AV,EN}$  has the second proportion of the total exergy destruction of the CTM process, 43.55 %. The splitter (FS), distillation column (RAD), and methanol synthesis reactor (R) have the largest proportion of the total unavoidable endogenous of the CTM process as shown in Fig. 8(c). Thus, optimization of the performance of these components have the largest impact on the reduction of the avoidable exergy destruction of the CTM process. The proportion of the  $E_{D,tot}^{UN,EX}$  and  $E_{D,tot}^{AV,EX}$  of the CTM process is less than 5 % due to the CTM process has little exogenous exergy destruction. The former is mainly caused by the splitter (FS), heat recovery cooler (EX5) and methanol synthesis reactor (R); the latter is by raw gas preheating exchanger (EX6) and raw gas heater (HX), as shown in Fig. 8(d) and (e). Considering the unavoidable and avoidable exogenous exergy destruction is relatively small, the interrelationship of the components has less impact on the reduction of the exergy destruction of the CTM process in comparison with that of the components themselves. Therefore, more efforts should be focused on the reduction of the avoidable endogenous exergy destruction of the CTM process, especially the components with high avoidable endogenous exergy destruction.

#### 4.4. Key parameters optimization and improvement strategies development

As mentioned above, the proportion of the endogenous avoidable exergy destruction of the CTM process is much higher than that of the exogenous exergy destruction. Therefore, this study is focused on the reduction of the endogenous exergy destruction which is caused by the components themselves, especially the splitter (FS) and distillation column (RAD) because of their highest avoidable exergy destruction.

##### 4.4.1. Reduction of avoidable exergy destruction of the splitter

Due to the splitter has the highest endogenous avoidable exergy destruction, the recycle ratio of this component is firstly optimized as shown in Fig. 9(a) and (b). Increasing the recycle ratio means more and more unreacted gas is recycled to the methanol synthesis reactor. As a result, the output methanol is quickly increased from 605.19 kmol/h to 787.56 kmol/h when the recycle ratio is increased from 0.90 to 0.98, but it slightly increases when the ratio is higher than 0.98. However, the energy consumption of the recycle compressor is greatly increased from 7.9 MW to 11.5 MW when the recycle is increased from 0.9 to 1.0 as shown in Fig. 9(a). In addition, the avoidable and total exergy destruction of the CTM process are gradually decreased when the unreacted gas recycle ratio is increased from 0.9 to 0.98. It is mainly because of the increasement of the output methanol and total conversion



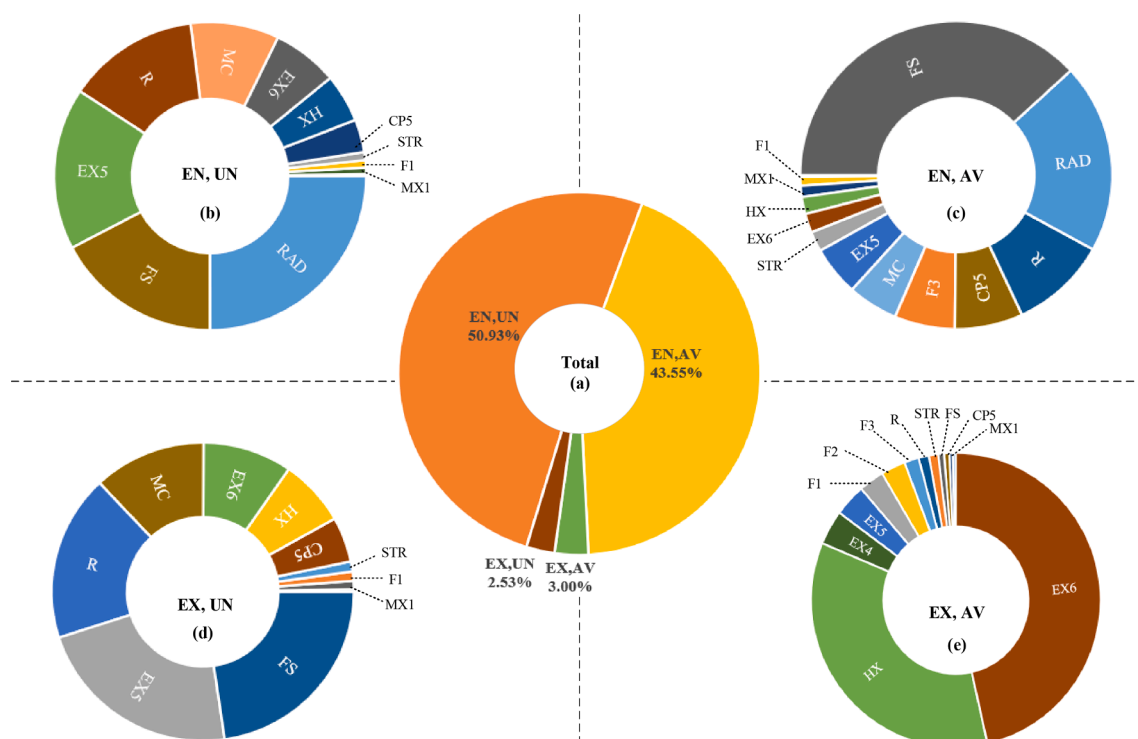


Fig. 8. Combination of splitting the exergy destruction of the CTM process.

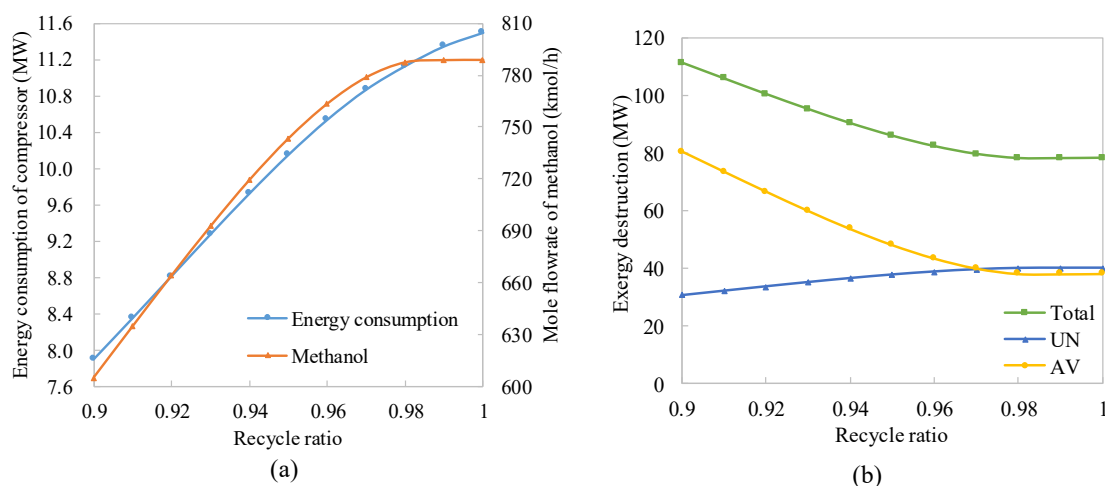


Fig. 9. Effect of the recycle ratio on the performance of the CTM process.

ratio of raw syngas as shown in Fig. 9(b). But these two exergy destructions do not change when the recycle ratio is higher than 0.98. However, due to the irreversibility of the compressor and related components, the unavoidable exergy destruction of the CTM process is obviously increased along with the increasement of the recycle ratio. Thus, to reduce the avoidable exergy of the splitter, the recycle ratio is recommended to be about 0.98.

#### 4.4.2. Reduction of avoidable exergy destruction of the distillation column

The avoidable exergy destruction of the distillation column accounts for 67.96 % of its total exergy destruction. The effect of total number of theoretical stages and feed stage on the heat duty of the reboiler, mole flowrate of methanol, and exergy destruction of the distillation column are indicated in Fig. 10(a)–(d). As Fig. 10(a) shown, the methanol out

from the top of the distillation column is greatly increased from 769.96 kmol/h to 787.56 kmol/h with a design specification, and the heat duty of the reboiler is greatly reduced from 15.6 MW to 14.4 MW when the total number of theoretical stages is added from 25 to 30. However, both the mole flowrate of methanol and heat duty of reboiler are slightly changed when the number of theoretical stages is more than 30. Due to most of the target methanol is recovered from the top of the distillation column when the total number of theoretical stages is about 30, the total and avoidable exergy destruction of the distillation column are greatly decreased firstly along with the increasement of the total number of theoretical stages; however, when it is larger than 30, the total and avoidable exergy destruction are slightly decreased as shown in Fig. 10 (b). Therefore, the total number of theoretical stages of the distillation column are suggested to be about 30.

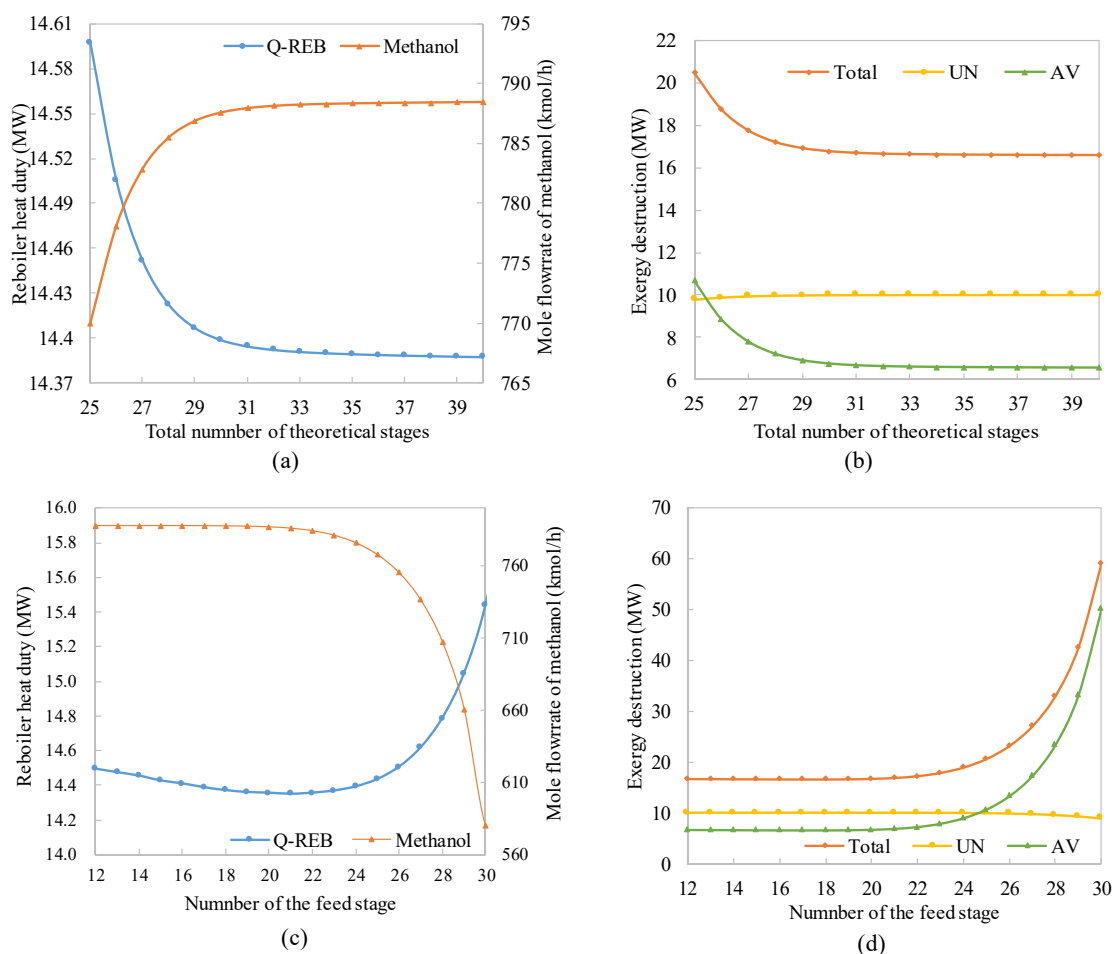


Fig. 10. Effect of the number of theoretical and feed stages on the performance of distillation column.

Changing the number of the feed stage of the distillation column will significantly affect its output methanol, reboiler heat duty, and exergy destruction as shown in Fig. 10(c) and (d). When the number of the feed stage of the distillation column is lower than 22, its output methanol, reboiler heat duty, and exergy destruction are changed slightly, but the output methanol is significantly decreased when the number of the feed stage is higher than 22. In addition, the reboiler heat duty, total and avoidable exergy destruction are significantly increased when the number of the feed stage is higher than 22. Thus, the number of the feed stage of the distillation column is recommended to be 22 in this work.

#### 4.4.3. Comparison of the optimized and reference CTM processes

To illustrate the merits of the above proposed improvement strategies, the optimized CTM process is compared with the benchmark case as shown in Fig. 11. The avoidable exergy destruction of the optimized CTM process is decreased from 36.5 MW to 24.9 MW, but the unavoidable exergy destruction is almost unchanged. It is mainly because that optimization of the key operational parameters of the components of the CTM process can only reduce its avoidable exergy destruction but have little impact on its unavoidable exergy destruction. As a result, the total exergy destruction of the CTM process is reduced from 78.5 MW to 66.9 MW, and the exergy efficiency is improved from 66.62 % to 71.53 %, respectively. Therefore, the proposed improvement strategies can obviously enhance the thermodynamic performance of the CTM process.

## 5. Conclusions and limitations

This study aims to ascertain the real improvement potential and

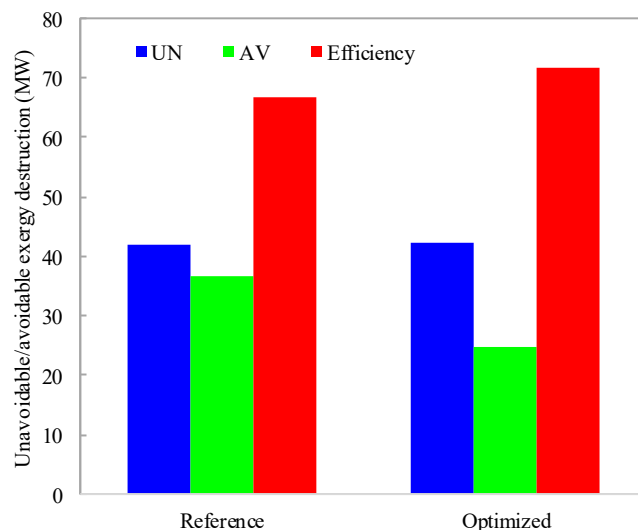


Fig. 11. Comparison the thermodynamic performance of the reference and optimized CTM process.

interactions between components of the CTM process by conducting an advanced exergy analysis. Although conventional exergy analysis can determine that the total exergy destruction ratio of the CTM process is 33.38 %, it fails to further determine the endogenous, exogenous,

avoidable and unavoidable exergy destruction of the CTM process. The following conclusions are obtained by employing the advanced exergy analysis method:

- The endogenous exergy destruction accounts for 94.47 % of the total exergy destruction of the CTM process. Thus, most of the exergy destruction of the components are caused by their own irreversibility, and their interactions have little impact on their exergy destruction.
- The real improvement potential of the CTM process is 46.55 % for exergy destruction reduction. 53.45 % of the exergy destruction cannot be reduced for the technical or economic limitations. More efforts should be paid to reduce the avoidable exergy destruction of the splitter, distillation column, and methanol synthesis reactor because they have the highest avoidable exergy destruction.
- The unavoidable endogenous exergy destruction of the CTM process has the largest proportion of its total exergy destruction, 50.93 %, followed by avoidable endogenous exergy destruction, 43.55 %. The proportion of the unavoidable and avoidable exergy destruction of the CTM process is less than 5 %.
- The total exergy destruction of the CTM process is reduced from 78.5 MW to 66.9 MW, and the exergy efficiency is improved from 66.62 % to 71.53 % after the recycle ratio of the unreacted gas, the total number of theoretical stages and feed stage of the distillation column are optimized.

Due to advanced exergy analysis method tends to pursue the minimum exergy destruction and optimum thermodynamic performance, it may add production cost and equipment investment. Hence, an economically infeasible although thermodynamically effective CTM process could be proposed. To address these limitations, an advanced exergoeconomic analysis with the goal of minimizing the total avoidable exergy cost, which combines the advantages of exergy and economic analyses, can be performed in terms of the results of advanced exergy analysis method in the future.

#### CRedit authorship contribution statement

**Qingchun Yang:** Conceptualization, Funding acquisition, Formal analysis. **Zhi Zhang:** Visualization, Formal analysis, Writing – review & editing. **Yingjie Fan:** Methodology, Writing – original draft, Investigation. **Genyun Chu:** Methodology, Data curation, Project administration. **Dawei Zhang:** Visualization, Formal analysis, Writing – review & editing. **Jianhua Yu:** Software, Resources, Writing – review & editing.

#### Declaration of Competing Interest

The authors declare that they have no known competing financial interests or personal relationships that could have appeared to influence the work reported in this paper.

#### Acknowledgements

The authors are grateful for financial support from the National Natural Science Foundation of China (No. 22108052) and the Fundamental Research Funds for the Central Universities (No. JZ2021HG7B0117).

#### Appendix A. Supplementary data

Supplementary data to this article can be found online at <https://doi.org/10.1016/j.fuel.2022.124944>.

#### References

- [1] Bakhtyari A, Mofarahi M, Lee CH. CO<sub>2</sub> adsorption by conventional and nanosized zeolites. *Advances in carbon capture*. Woodhead Publishing 2020:193–228.
- [2] Chen JM. Carbon neutrality: Toward a sustainable future. *The Innovation* 2021;2(3):100127.
- [3] Lane J, Greig C, Garnett A. Uncertain storage prospects create a conundrum for carbon capture and storage ambitions. *Nat Clim Change* 2021;11(11):925–36.
- [4] Van-Dal ES, Bouallou C. Design and simulation of a methanol production plant from CO<sub>2</sub> hydrogenation. *J Cleaner Prod* 2013;57:38–45.
- [5] Kotowicz J, Węcel D, Brzeczek M. Analysis of the work of a “renewable” methanol production installation based on H<sub>2</sub> from electrolysis and CO<sub>2</sub> from power plants. *Energy* 2021;221:119538.
- [6] González-Garay A, Frei MS, Al-Qahtani A, Mondelli C, Guillén-Gosálbez G, Pérez-Ramírez J. Plant-to-planet analysis of CO<sub>2</sub>-based methanol processes. *Energy Environ Sci* 2019;12(12):3425–36.
- [7] Kiss AA, Pragt JJ, Vos HJ, Bargeman G, de Groot MT. Novel efficient process for methanol synthesis by CO<sub>2</sub> hydrogenation. *Chem Eng J* 2016;284:260–9.
- [8] Wang J, Tang C, Li G, Han Z, Li Z, Liu H, et al. High-Performance M<sub>a</sub>ZrO<sub>x</sub> (M<sub>a</sub> = Cd, Ga) Solid-Solution Catalysts for CO<sub>2</sub> Hydrogenation to Methanol. *ACS Catal* 2019;9(11):10253–9.
- [9] Dang S, Qin B, Yang Y, Wang H, Cai J, Han Y, et al. Rationally designed indium oxide catalysts for CO<sub>2</sub> hydrogenation to methanol with high activity and selectivity. *Sci Adv* 2020;6(25):2060–77.
- [10] Zou T, Araújo TP, Krumeich F, Mondelli C, Pérez-Ramírez J. ZnO-promoted inverse ZrO<sub>2</sub>-Cu catalysts for CO<sub>2</sub>-based methanol synthesis under mild conditions. *ACS Sustainable Chem Eng* 2022;10(1):81–90.
- [11] Bai ST, De Smet G, Liao Y, Sun R, Zhou C, Beller M, et al. Homogeneous and heterogeneous catalysts for hydrogenation of CO<sub>2</sub> to methanol under mild conditions. *Chem Soc Rev* 2021;50(7):4259–98.
- [12] Frei MS, Capdevila-Cortada M, García-Muelas R, Mondelli C, López N, Stewart JA, et al. Mechanism and microkinetics of methanol synthesis via CO<sub>2</sub> hydrogenation on indium oxide. *J Catal* 2018;361:313–21.
- [13] Wang J, Zhang G, Zhu J, Zhang X, Ding F, Zhang A, et al. CO<sub>2</sub> Hydrogenation to Methanol over In<sub>2</sub>O<sub>3</sub>-Based Catalysts: From Mechanism to Catalyst Development. *ACS Catal* 2021;11(3):1406–23.
- [14] Cui Z, Meng S, Yi Y, Jafarzadeh A, Li S, Neyts EC, et al. Plasma-Catalytic Methanol Synthesis from CO<sub>2</sub> Hydrogenation over a Supported Cu Cluster Catalyst: Insights into the Reaction Mechanism. *ACS Catal* 2022;12(2):1326–37.
- [15] Seidel C, Jörke A, Vollbrecht B, Seidel-Morgenstern A, Kienle A. Kinetic modeling of methanol synthesis from renewable resources. *Chem Eng Sci* 2018;175:130–8.
- [16] Ghosh S, Sebastian J, Olsson L, Creaser D. Experimental and kinetic modeling studies of methanol synthesis from CO<sub>2</sub> hydrogenation using In<sub>2</sub>O<sub>3</sub> catalyst. *Chem Eng J* 2021;416:129120.
- [17] Zhang J, Li Z, Zhang Z, Liu R, Chu B, Yan B. Techno-economic analysis of integrating a CO<sub>2</sub> hydrogenation-to-methanol unit with a coal-to-methanol process for CO<sub>2</sub> reduction. *ACS Sustainable Chem Eng* 2020;8(49):18062–70.
- [18] Ahmed U. Techno-economic analysis of dual methanol and hydrogen production using energy mix systems with CO<sub>2</sub> capture. *Energy Convers Manage* 2021;228:113663.
- [19] Harris K, Grim RG, Huang Z, Tao L. A comparative techno-economic analysis of renewable methanol synthesis from biomass and CO<sub>2</sub>: Opportunities and barriers to commercialization. *Appl Energy* 2021;303:117637.
- [20] Özcan HG, Varga S, Gunerhan H, Hepbasli A. Numerical and experimental work to assess dynamic advanced exergy performance of an on-grid solar photovoltaic-air source heat pump-battery system. *Energy Convers Manage* 2021;227:113605.
- [21] Wiesberg IL, Brigagão GV, de QF Araújo O, de Medeiros JL. Carbon dioxide management via exergy-based sustainability assessment: Carbon Capture and Storage versus conversion to methanol. *Renew Sustain Energy Rev* 2019;112:720–32.
- [22] Açıkkalp E, Caliskan H, Altuntas O, Hepbasli A. Novel combined extended-advanced exergy analysis methodology as a new tool to assess thermodynamic systems. *Energy Convers Manage* 2021;236:114019.
- [23] Yang X, Yang S, Wang H, Yu Z, Liu Z, Zhang W. Parametric assessment, multi-objective optimization and advanced exergy analysis of a combined thermal-compressed air energy storage with an ejector-assisted Kalina cycle. *Energy* 2022;239:122148.
- [24] Song M, Zhuang Y, Zhang L, Wang C, Du J, Shen S. Advanced exergy analysis for the solid oxide fuel cell system combined with a kinetic-based modeling pre-reformer. *Energy Convers Manage* 2021;245:114560.
- [25] Yuan B, Zhang Y, Du W, Wang M, Qian F. Assessment of energy saving potential of an industrial ethylene cracking furnace using advanced exergy analysis. *Appl Energy* 2019;254:113583.
- [26] Wu J, Wang Na. Exploring avoidable carbon emissions by reducing exergy destruction based on advanced exergy analysis: A case study. *Energy* 2020;206:118246.
- [27] Somers C, Mortazavi A, Hwang Y, Radermacher R, Rodgers P, Al-Hashimi S. Modeling water/lithium bromide absorption chillers in ASPEN Plus. *Appl Energy* 2011;88(11):4197–205.
- [28] Liang B, Ma J, Su X, Yang C, Duan H, Zhou H, et al. Investigation on deactivation of Cu/ZnO/Al<sub>2</sub>O<sub>3</sub> Catalyst for CO<sub>2</sub> hydrogenation to methanol. *Ind Eng Chem Res* 2019;58(21):9030–7.
- [29] Asif M, Gao X, Lv H, Xi X, Dong P. Catalytic hydrogenation of CO<sub>2</sub> from 600 MW supercritical coal power plant to produce methanol: A techno-economic analysis. *Int J Hydrogen Energy* 2018;43(5):2726–41.

- [30] Tsatsaronis G, Morosuk T. Advanced exergetic analysis of a refrigeration system for liquefaction of natural gas. *Int J Energy Environ Eng* 2010;1(1):1–18.
- [31] Yu Y, Li B, Fang Z, Wang C. Energy and exergy analyses of pellet smelting systems of cleaner ferrochrome alloy with multi-energy supply. *J Cleaner Prod* 2021;285: 124893.
- [32] Yang Q, Qian Y, Kraslawski A, Zhou H, Yang S. Advanced exergy analysis of an oil shale retorting process. *Appl Energy* 2016;165:405–15.
- [33] Kelly S, Tsatsaronis G, Morosuk T. Advanced exergetic analysis: Approaches for splitting the exergy destruction into endogenous and exogenous parts. *Energy* 2009;34(3):384–91.
- [34] Ambriz-Díaz VM, Rubio-Maya C, Ruiz-Casanova E, Martínez-Patiño J, Pastor-Martínez E. Advanced exergy and exergoeconomic analysis for a polygeneration plant operating in geothermal cascade. *Energy Convers Manage* 2020;203:112227.
- [35] Li L, Liu Z, Deng C, Ren J, Ji F, Sun Yi, et al. Conventional and advanced exergy analyses of a vehicular proton exchange membrane fuel cell power system. *Energy* 2021;222:119939.
- [36] Liu X, Yan X, Liu X, Liu Z, Zhang W. Comprehensive evaluation of a novel liquid carbon dioxide energy storage system with cold recuperator: Energy, conventional exergy and advanced exergy analysis. *Energy Convers Manage* 2021;250:114909.
- [37] An X, Zuo Y, Zhang Q, Wang J. Methanol Synthesis from CO<sub>2</sub> Hydrogenation with a Cu/Zn/Al/Zr Fibrous Catalyst. *Chin J Chem Eng* 2009;17(1):88–94.